SRTTU

Journal of Electrical and Computer Engineering Innovations

JECEI, Vol. 4, No. 1, 2016

Regular Paper

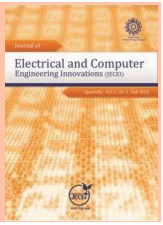

Research of Low Voltage Shore Power Supply Used on Shipping Based on Sliding Control

Guoliang Yang[1,*], Yanxiao Jia[1], ManCuiHang Qin[1], and Yiming Fang[1]

[1] Key Lab of Power Electronicsfor Energy Comservation and Motor Driveof Hebei Province, YanShan University, Qinhuangdao, China.

*Corresponding Author's Information: y99ygl@ysu.edu.cn

ARTICLE INFO

ARTICLE HISTORY:
Received 13 December 2016
Revised 25 January 2017
Accepted 25 January 2017

KEYWORDS:
SPS
Diode-clamped Three-level Inverter
Sliding Control
SVPWM

ABSTRACT

In order to solve the problem of fuel pollution, the diesel fuel for power generation of marine was abandoned and shore power supply have been proposed at the historic moment. The Shore Power Supply which needs transferring 380V/50Hz to 450V/60Hz is used on shipping who need this kind of power, so effectively curbs the emissions of pollution gas into the air, and achieves the purpose of improving the environment. At the same time, in order to achieve better control, in this paper, sliding mode control is applied to the closed loop system. The structure of the main circuit, drive circuit and control system are described and the design of critical parameters are provided.

1. INTRODUCTION

With the environmental problem becoming more and more serious, the fuel pollution has gradually been taken seriously. The ships generally use diesel generating units to generate electricity, causing serious pollution to the air port. In addition, with the continuous expansion of foreign trade, more and more foreign merchant ships operate in our ports. Most foreign ships use 450VAC/60Hz [1], while the standard of China's electric power industry is 380VAC/50Hz. Although the traditional diesel generator can produce 450VAC/60Hz, it has lots of disadvantages such as causing noise and air pollution, low efficiency, etc. The shore power supply (SPS) of the low voltage ship mentioned in this paper no longer needs the diesel generator to generate electricity. Instead, the AC-DC-AC power electronic transformation technology is used to transfer alternating current of 380V/50Hz to 450V/60Hz directly, so that provides power to such electric ships.

2. THE OPERATING PRINCIPLE OF SHORE POWER SUPPLY

The shore power supply is mainly composed of two parts, power conversion circuit and control circuit [2]. The part of power conversion is aimed at energy transfer and conversion, which means that it can convert alternating current of three-phase of 380V/50Hz to 450V/60Hz (Fig. 1). The part of control circuit is mainly based on the state of the detected signal to make judgment processing, achieving the goal of shore power supply system control and protection.

A . Design of the Main Circuit

The main circuit topology of shore power supply mentioned in this paper is shown in Fig. 2. Rectifier filter circuit adopts three-phase non-controlled rectifier. DC reactor have the advantage of reducing the harmonic of the current of input side, smoothing the output voltage and reducing the current ripple in DC side, providing a relatively stable DC voltage for the later stage inverter.

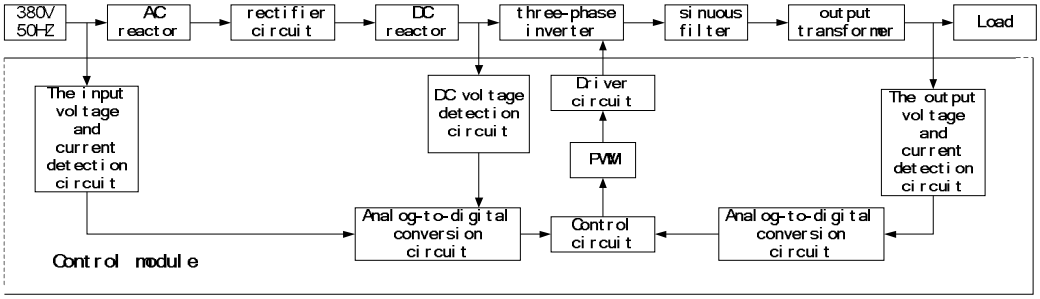

Figure 1: The structure of shore power supply.

The application of diode-clamped inverter increases the flexibility of input voltage of the shore power supply, at the same time contributes to the versatility design of the shore power supply and improves waveform quality of the output voltage. Filter which is the key component in the inverter system, convert PWM wave of the output to sine wave and smooth the inverter AC voltage to guarantee the good quality of power supply system. The output transformer on shore power supply has play an important role in voltage transformation and isolation protection.

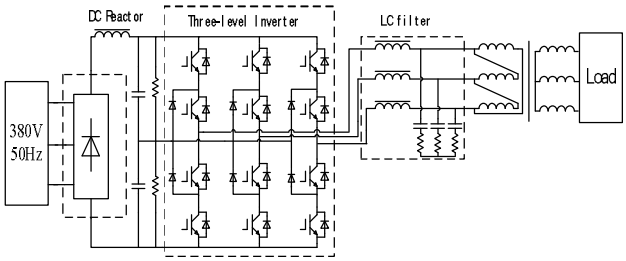

Figure 2: Main circuit topology of shore power supply.

Assuming that the voltage of DC side is 530V when the output power is 8kW, then the equivalent output current is 15.1A and the equivalent load is 35.1Ω in the DC side. The critical conditions of current continuity of DC side are:

$$\omega\tau \geq 0.009142 \tag{1}$$

where τ is the time constant, $\tau = L/R$, L is the filtering inductance in DC side, R is the equivalent resistance in DC side. In fact, once the current in the circuit is continuous, the power factor of net side is greater than 0.8. So, choosing the inductance according to $\omega\tau \geq 0.02 \sim 0.04$ is more appropriate. At this time, the power factor is between 0.91 ~ 0.94. If continually add the inductance value, will only increases the cost and equipment weight of the system, but not improves the power factor [3].

The calculation equation of the inverter output filter inductance and the calculation equation of filter capacitance are presented in (2) and (3) respectively [4].

$$L = \sqrt{\frac{(\frac{\omega U_o^2}{\omega_c^2} + \frac{\omega^3 U_o^2}{\omega_c^4})}{\omega I_o^2}} \tag{2}$$

$$C = \frac{1}{\omega_c^2} \times \sqrt{\frac{\omega I_o^2}{(\frac{\omega U_o^2}{\omega_c^2} + \frac{\omega^3 U_o^2}{\omega_c^4})}} \tag{3}$$

where U_0 is the RMS of the inverter output voltage, w_c is the cut-off angular frequency and I_0 is the RMS of phase current for inverter output. Assuming the voltage of the DC bus is 530V at full load, so, the peak value of output phase voltage of the inverter is 265V. If the modulation ratio is 0.8, the valid value of the output phase voltage is 150V. The output voltage fundamental wave angle frequency of the shore power is $\omega_0 = 120\pi\ rad/s$, the cut-off angle frequency is $\omega_c = 2000\pi\ rad/s$, then the output phase current is 17.8A when the output power is 8 kW.

Assuming that the output phase voltage of the inverter is 150V and take those values into the (2) and (3), then the value of inductance and capacitance can be obtained as L=1.34mH and C=18.9uF and the actual value of inductance and capacitance is 1.44mH and 17.6uF in each phase respectively.

The two level inverter of traditional system is applied in the high voltage and high power applications, as the limitation of semiconductor device for itself, generally improve the switch tube level of pressure and flow capacity by adapting the way of switching device in series-parallel, which requires the combined switch tube can be opened and shut off at the same time.

However, due to the restrictions of the semiconductor devices and manufacturing process, exactly matching between devices has certain

difficulty. So, multilevel inverter has been widely researched and applied. But as the circuit of more than three level of three-phase inverter is complex, it is difficult to reduce electromagnetic interference caused by stray inductance, and its shut off voltage peak has been increased, which all lead to the pressure of the system on the device level requirements.

So, the most widely used at present is mainly three-level inverter.

Diode-clamped three-level inverter circuit which is wildly used inverter, have the advantage of its simple structure, without complex transformer, relatively simple control circuit and control method [5]. Fig. 2 shows the diagram of the diode-clamped three-level inverter circuit.

The value of three-phase sinusoidal voltage instantaneous corresponding to the reference space voltage vector is defined as:

$$v_{\text{ref}} = \frac{2}{3}(v_{\text{a}} + v_{\text{b}}e^{\text{j}\frac{2\pi}{3}} + v_{\text{c}}e^{-\text{j}\frac{2\pi}{3}}) \tag{4}$$

Since each phase of three-level inverter has three kinds of switch state (i.e., S_i=(1,0,-1), therefore, a three-phase three-level inverter can output 27 kinds of state, in turn can get a voltage vector space vector diagram contains 27 voltage vector spaces (Fig.3). According to the magnitude of voltage vector, it can be divided into zero vector, small vector, medium vector, and large vector in which the magnitude of the large vector is 2Vdc/3, the amplitude of the middle vector is Vdc/3, and the amplitude of the zero vector is zero [6].

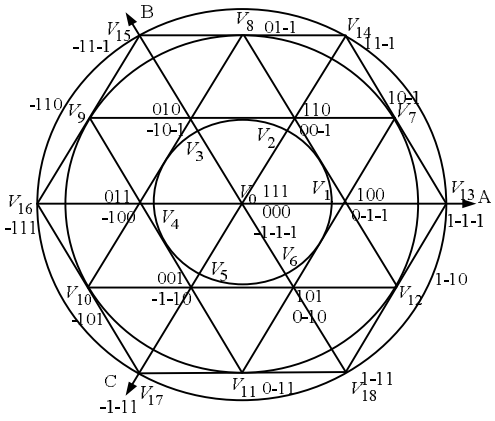

Figure 3: The block diagram of three-phase three-level space vector.

To achieve three-level inverter, SVPWM control generally takes four steps: (1) to judge the large sectors; (2) to judge the small sector; (3) to calculate the duration of action of each synthetic vector; (4) to assign time state. The sequence of switching states follows the following principle: Starting from the negative small vector, only one phase of the switching state is changed at time, and when the switching state is switched from 1 to -1, the switch state 0 must as the transition working state [7], [8].

B. The Design of Snubber Circuit

Whereas the IGBT works in a higher switching frequency or larger power occasions, due to the presence of stray inductance in the main circuit, the IGBT bear a larger surge voltage at the turn-off moment [9]. This will inevitably lead to greater switching losses of IGBT, thus, making IGBT overheating and even cause IGBT damage. In order to improve the reliability of IGBT, generally can reduce the switching speed, reduce the number of the stray inductance in the circuit and add the snubber circuit to suppress the surge voltage at the turn-off moment and reduce the switching losses. As the slower switching speed will increase the switching losses to a certain extent, so the most effective way is to reduce the stray inductance through the compact wiring and use the buffer circuit to suppress the shutdown surge voltage. Take the phase A of the three-level inverter as an example, the connection form of the RCD absorption circuit is shown in Fig. 4. The specific working process can be referred to [10].

At the same time, as the existence of mid-point bus stray inductance, result the voltage imbalance of both inside and outside in three-level inverter when the switch turn off, generally the voltage that the inner switch bears is slightly higher than the outer switch. In order to balance the switch-off voltage of the inner and outer switch, generally a resistor Ra is connected in parallel between the clamping diodes in engineering, as shown in Fig. 4. Thus, the capacitor in DC side can charge the junction capacitance of Sa4 via the D1 and Ra which generally take Ra=10k in engineering. Of course, the introduction of resistance Ra will bring additional losses to a certain extent and increase the difficulty in the design of the system thermal.

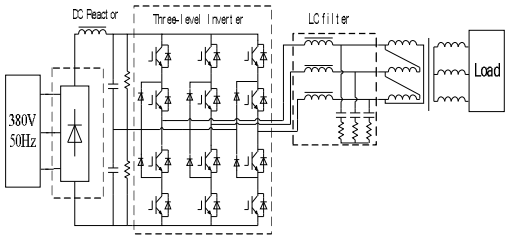

Figure 4: Three-level inverter with snubber circuit.

C. The Design of Drive Circuit

The drive circuit converts the SVPWM signal generated by the DSP into a signal capable of driving

the IGBT, select IR2113 as driver chip. The signal input and output of IR2113 is no isolation, so the PWM signal generated by the DSP is sent to the IR2113 signal input after electrical isolation, making the PCB-grounding of the control circuit and the main circuit isolate to improve system reliability. Select 6N137 as optocoupler isolation [11], [12], the circuit structure is shown in Fig. 5.

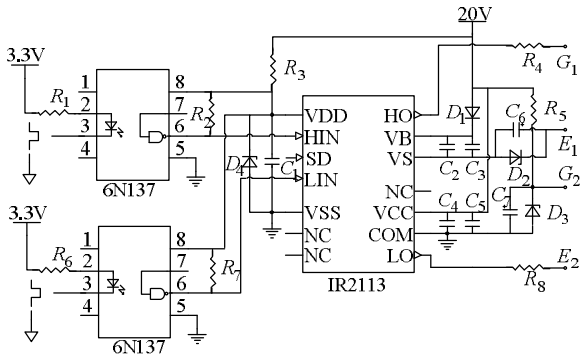

Figure 5: Schematic diagram of drive circuit.

D. The Control Structure of the System

Sliding mode control (SMC) is one of variable structure control modes. It is a special nonlinear control with discontinuous characteristics [13]. The system structure of this control strategy changes according to the switching characteristic during the control process, forcing the system state slide to the equilibrium point along a certain hyper plane and asymptotically achieve a steady state at this point or near it. This state is the so-called sliding mode, and the sliding mode variable structure control system is a variable structure control system with sliding mode.

As soon as the system enters the sliding mode, the sliding mode motion is almost independent with the disturbance or parameter, so the sliding mode control is robust and easy to implement. In recent years, it has been applied in the closed-loop speed control system of synchronous motor and obtained excellent control performance.

A nonlinear system is provided as follows:

$$\dot{x} = f(x,u,t) \tag{5}$$

where $x \in R^n$, $u \in R^m, n > m$ and the control function is:

$$u_i(x) = \begin{cases} u_i(x)^+ & s_i(x) > 0 \\ u_i(x)^- & s_i(x) < 0 \end{cases} \tag{6}$$

where $u_i(x)^+ \neq u_i(x)^-$, $s = s(x)$ is the toggle function which its dimension is the same as the control vector. Then, a hyper plane is constructed, and divides the system into two parts. Therefore, this hyper plane is called the switching surface.

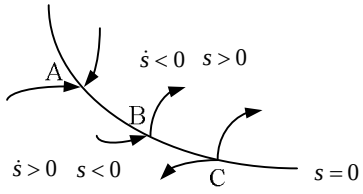

Figure 6: The figure of switching surface.

As shown in Fig. 6, point A approaching from both sides to switching surface is called the end point; point B passing the plane to the other side after reaching the switching surface is called the ordinary point; point C leaving from the switching surface to the both sides is called the starting point.

The termination point has the most special meaning among the three categories. A region where only have an termination point on and the motion trajectory of the system also simultaneously tends to is called “sliding mode region” and the motion in this region is called “sliding motion”.

Change the structure of the system by changing the state of switches on both sides of $s(x) = 0$, when the system is in sliding mode, there is $s(x) = 0$, $\dot{s}(x) = 0$. Make the system meet the three basic conditions at the same time, namely the existence, accessibility and stability by selecting appropriate switching function $s(x)$ and control signal $u(x)$.

The existence condition of the system is:

$$\lim_{s \to 0} s\frac{ds}{dt} \leq 0 \tag{7}$$

The reachability condition of the system is:

$$s\frac{ds}{dt} < 0 \tag{8}$$

It can be seen from Fig. 6 that (7) can be equivalent to (8). Therefore, (8) is the reachability condition of the sliding mode, and it can also be used as the existence condition of the sliding mode.

The stability of the sliding mode motion is also needed to satisfy while reach the existence and reachability conditions. Under normal circumstances, stability analysis can be carried out according to Lyapunov theory.

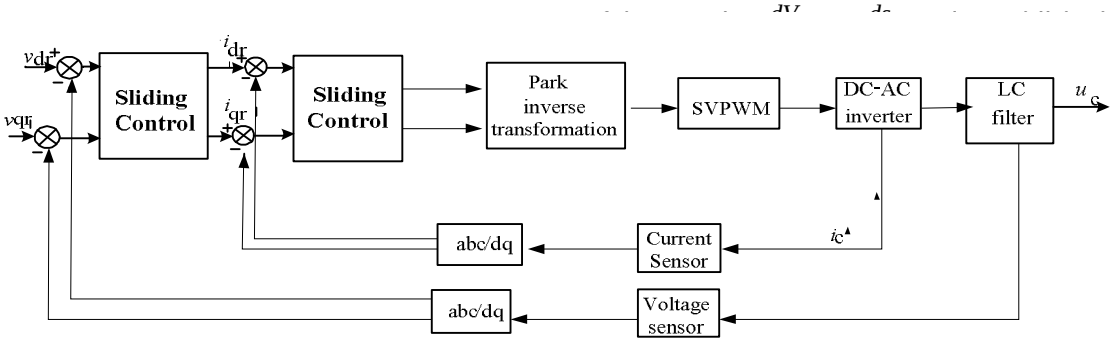

Figure 7: The block diagram of the system output .

The block diagram of three-phase inverter model under two phase rotating coordinate system is shown in Fig. 8.

According to Fig. 8, three-phase voltage source inverters in the dq coordinate system exist certain coupling. However, the analysis found that under the condition that the output voltage of the inverter is symmetric, the d-axis component of the three-phase inverter output voltage is a direct current, which is the amplitude of phase voltage under the three-phase static coordinate system, and the q-axis component is 0.

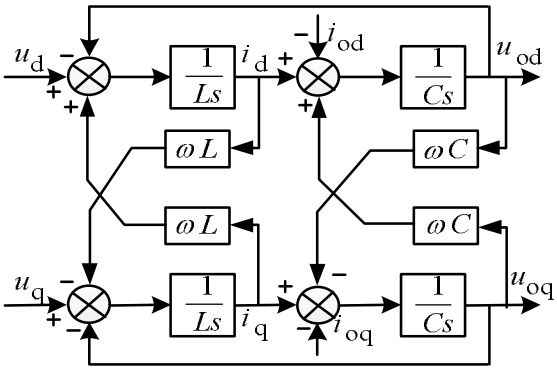

Figure 8: The model diagram of three-phase inverter in the dq coordinate system.

In this case, there is no coupling between the dq es, which facilitates the control of the inverter. The ock diagram of voltage and current double-closed loop control system based on the capacitor in the dq coordinate system is shown in Fig. 9. The positive definite Lyapunov function is constructed as follows:

$$V = \frac{1}{2} \quad (\varsigma^T s)$$

(9)

Since the control system of sliding mode of variable structure has the characteristics of adaptive, good dynamic quality, strong robustness and good steady-state performance, the controller structure of shore power supply adapts sliding mode control. The block diagram of the system output control is shown in Fig. 7.

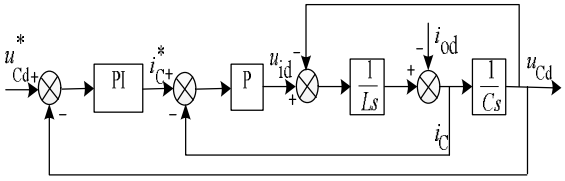

Figure 9: The control diagram of the voltage and current of capacitance of double closed loop control.

The transfer function of PI regulator is $W_{vc} = K_1 + K_2 / S$, $W_{ic} = K_3$ respectively and then the closed-loop transfer function of the current is :

$$D(s) = LCs^3 + K_3Cs^2 + (K_1K_3 + 1)s + K_2K_3 \quad (10)$$

The closed-loop transfer function of the double closed-loop control system is:

$$G(s) = \frac{K_1K_3s + K_2K_3}{LCs^3 + K_3Cs^2 + (K_1K_3 + 1)s + K_2K_3} \quad (11)$$

The closed-loop characteristic equation is:

$$D(s) = LCs^3 + K_3Cs^2 + (K_1K_3 + 1)s + K_2K_3 \quad (12)$$

The expected closed-loop dominant pole of the double-closed loop control system is $S_{1,2} = -\zeta\omega_n \pm j\omega_n\sqrt{1-\zeta^2}$, the non-dominant pole is

$S_3 = -n\zeta\omega_n$ and then the expected characteristic equation of the double-loop control system is :

$$D(s) = (s-s_1)(s-s_2)(s-s_3) = (s^2 + 2\zeta\omega_n + \omega_n^2)(s + n\zeta\omega_n) \quad (13)$$

Comparing and sorting out the equations (12) and (13), obtaining the equation:

$$K_1 = \frac{(1+2n\zeta^2)\omega_n^2 LC - 1}{K_3} \quad (14)$$

$$K_2 = \frac{n\zeta\omega_n^3 LC}{K_3} \quad (15)$$

$$K_3 = (2+n)\zeta\omega_n L \quad (16)$$

If expectation of damping ratio is $\zeta = 0.707$, the natural frequency is $K_3 = \omega_n = 1/\sqrt{LC} = 5655$ and n is 10. Adjusting its parameters can set $K_1 = 0.0927$, $K_2 = 552.67, K_3 = 85.39$.

The Bode diagram of the open-loop transfer function of the control system after adding the regulator is shown in Fig. 10. In order to obtain a satisfactory transient response, the general phase margin should be between 30 ° to 60 °, while the gain margin should be greater than 6dB. According to Fig. 11, it can be seen that the control system has good dynamic response speed and stability.

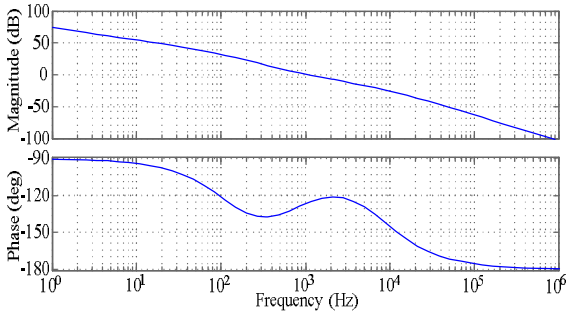

Figure 10: The Bode diagram of open-loop transfer function of control system with regulator.

In this paper, TMS320F2812 is adopted as processor [14]. The system software consists of the main program and interrupt subroutine (Fig. 9). Initialization is necessary preparation before programming. Initialization generally includes module initialization and variable initialization. This topic involves the initialization module mainly includes: CPU configuration initialization, PIE initialization, the I/O initialization, event manager initialization, ADC module initialization and so on. AD sampling is the key to achieve closed-loop control. ADC module settings include ADC power-up sequence settings, ADC clock and sampling period of the configuration, sampling and channel configuration and determine the conditions of analog to digital conversion.

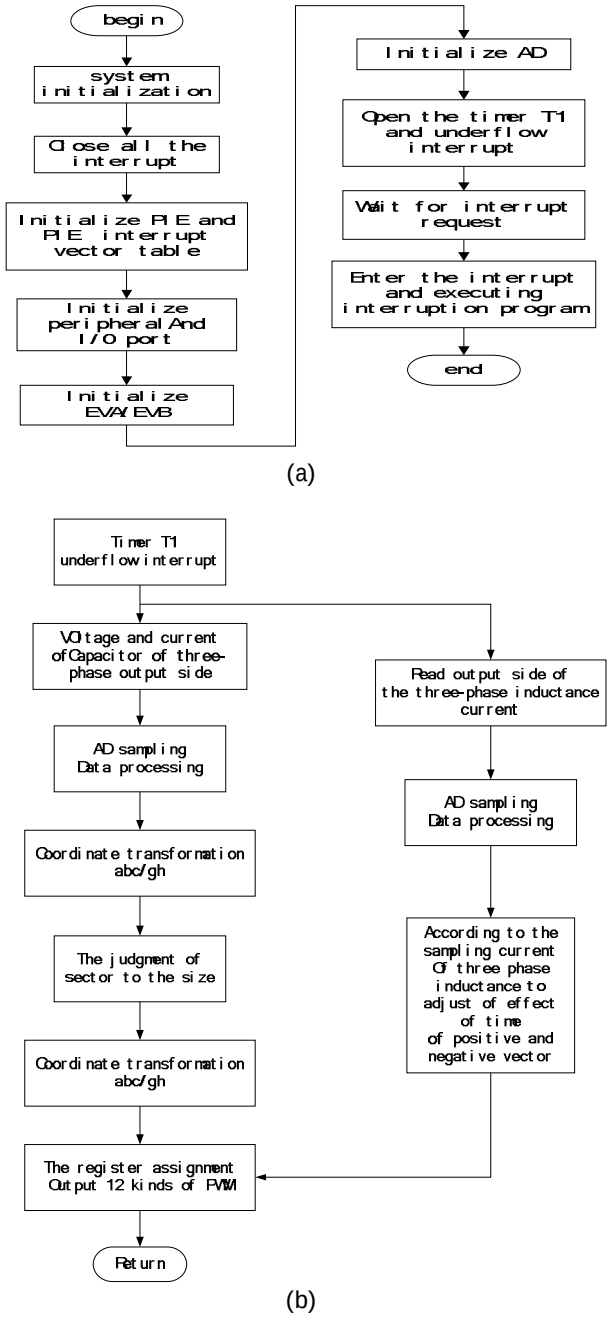

Figure 11: Flow chart of the system design.

3. Simulation and Experiment

In this paper, a system simulation model is established in Matlab/Simulink and an experimental platform is set up. The main electrical power performance indicators are shown in Table 1. The driving simulation waveform of phase A of three-level inverter is shown in Fig. 12.

Fig. 13 shows the changing of output voltage with different load when the open-loop and capacitor

voltage-current double-loop control is applied to the shore power supply.

TABLE 1
LOW VOLTAGE SHORE POWER SUPPLY PART OF THE ELECTRICAL PERFORMANCE

Name of parameter	Indication range
Three-phase input voltage	380V±10%
Input frequency	50HZ±2%
Input voltage	≤5%
Three-phase output voltage	450V±5%
Output frequency Output voltage	60HZ±2%
Change range of instantaneous voltage	≤5%

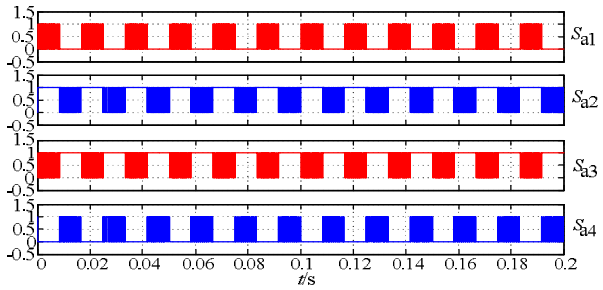

Figure 12: The simulation waveform of phase A driving.

Through the analysis, we found that the use of the feedback of current and voltage of the capacitance in double closed-loop control is good to improve the output external characteristic of inverter, and the same time to improve the ability and speed of dynamic response of the system.

Fig. 14 shows the THD value of the output voltage of the shore power supply. It can be seen that the THD is 0.7%, meeting the requirement that the THD value of shore power supply output voltage less than 5%.

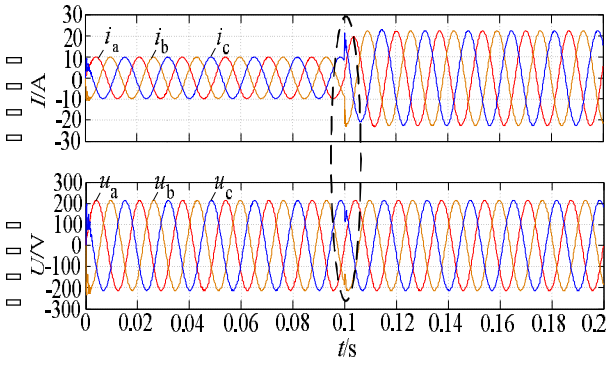

Figure 13: Output voltage simulation waveform for closed-loop load switching.

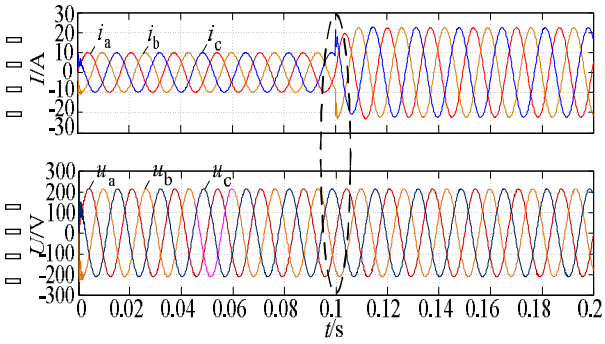

Figure 14: The THD value of the output voltage of the shore power supply.

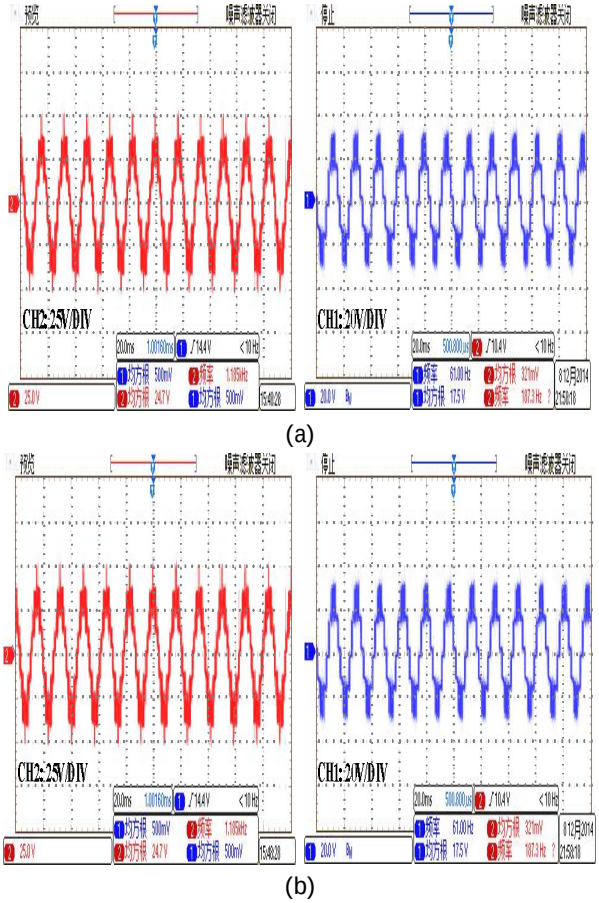

Figure 15: Experiment waveform of the voltage u_{AN} and the voltage u_{an}

The experimental output voltage waveform of the inverter to mid-point voltage of AC side is shown in Fig. 15(a) and the experimental output line voltage waveform of the inverter is shown in Fig. 15(b).

As shown in Fig. 16, CH1 is the experiment output voltage waveform of the inverter to the mid-point voltage of the DC side and CH2 is the experiment waveform of output voltage with filter.

Through the observation of the above experiment waveforms, we found that the output frequency of the

output voltage is 60 Hz, which meets the requirements of shore power supply.

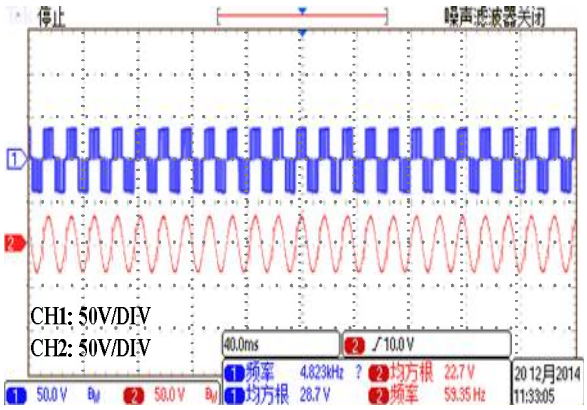

Figure 16: Experiment waveform of output voltage u_{An} of and the output voltage with filter.

The experimental waveforms of the AC output voltage (CH2) and the output current (CH1) of the phase A is shown in Fig. 17(a).

The AC output current is reduced to 1/100 of the original via the current transformer and the actual current is 1.74A, at this time, the RMS of output voltage is 17.4 V.

It can be also seen from the Fig. 17(b) that, the output current of phase A is 3.3A and the effective value of actual output voltage is 15.3 V.

However, the above two cases are measured when DC side voltage is 45V. After analysis, it can be found that when the load increases, the output voltage will fell. So, we can make sure that in the case of open loop, the capacity of carrying load of the shore power supply is insufficient.

Fig. 18 shows the experiment platform of shore power supply.

4. Conclusion

In this paper, the design principle is analyzed in details according to the topological structure and working principle of shore power supply and sliding mode control. According to the simulation and experiments, it is shown that the power quality of the shore power supply based on sliding mode control can meet the requirements of shore power supply.

5. Acknowledge

This project is supported by the National Natural Science Foundation of China under Grant No.U1260203, the Science and Technology project of Hebei province, China under Grant No.15214318, and the University research program of Xinjiang Uygur Autonomous Region, China under Grant No.XJEDU2016S114.

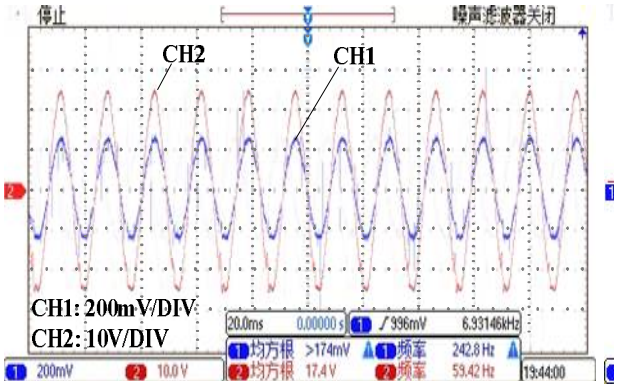

(a)

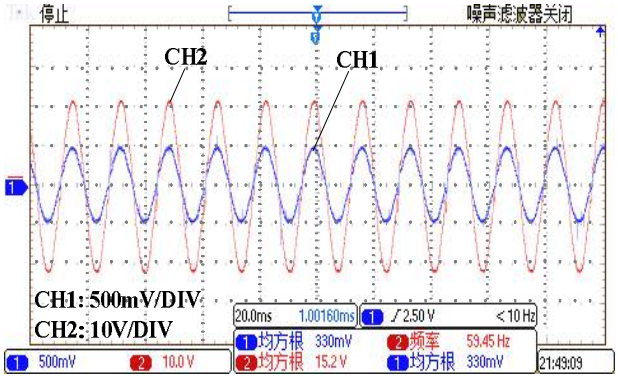

(b)

Figure 17: Experimental waveform of voltage and current of the AC output side.

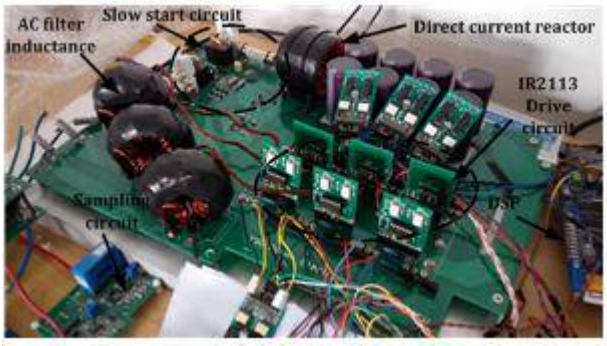

Figure 18: The experimental platform of shore power supply.

References

[1] X. Yang, G. Bai, and R. Schmidhalter, "Shore to ship converter system for energy saving and emission reduction," in *Proc.* 2011 *IEEE 8th International Conference on Power Electronics and ECCE Asia, pp.*2081-2086.

[2] H. Yang, "Brief introduction of shore shore system," *Jiangsu Ship*, vol. 28, no. 4, pp. 23-26, 2011.

[3] N. Yi, X. Tang, and Y. Peng, "Study on parameter optimization design of uncontrollable rectifier," *Power Electronics Technology*, vol. 41, no. 1, pp. 90-91, 2007.

[4] L. He and J. Wang, "Three-phase PWM inverter output LC filter design method," *Electric drive*, vol. 43, no. 12, pp. 33-36, 2013.

[5] J. Wang, B. Yang, and J. Zhao, "Development of a compact 750KVA three-phase NPC three-level universal inverter module with specifically designed busbar," in *Proc. 2010 IEEE Applied Power Electronics Conference and Exposition (APEC)*, *Twenty-Fifth Annual IEEE Conf*. pp. 1266-1271.

[6] H. Jin, Z. Bo, and L. Yang, "DSP-based implementation of a simple space vector pulse width modulation algorithm for three-level NPC inverter," in *Proc. 2011 IEEE 4th International Symposium on. Microwave, Antenna, Propagation, and EMC Technologies for Wireless Communications (MAPE),* pp. 726-729.

[7] M. Li, "Algorithm research and simulation of three-level SVPWM," M.S. dissertation, Dept. Hefei University of Technology, 2007: 2-15.

[8] H. Jin, Z. Bo, and L. Yang, "DSP-based implementation of a simple space vector pulse width modulation algorithm for three-level NPC inverter," Microwave, Antenna, Propagation, and EMC Technologies for Wireless Communications (MAPE), 2011 IEEE 4th International Symposium on. IEEE, 2011: 726-729.

[9] Z. Zhou and A. Ji, "IGBT drive and protection circuit design and applications circuit examples," Beijing: mechanical industry press, 2011:215-217.

[10] Z. Zhao, N. Wei, and B. Zhao, "General buffer circuit model and three-level IGBT converter internal and external component voltage imbalance mechanism," *Transactions of China Electrotechnical Society*, vol. 20, no. 6, pp. 30-34, 2000.

[11] F. Wanag and S. Zhang, "Hardware design of three - level inverter," *Marine Electric Technology*, vol. 30, no. 10, pp. 16-19, 2010.

[12] X. Gu, J. Yang, and Z. Zhang, "A novel three-phase three-level inverter," *Power Electronics Technology*, vol. 47, no. 5, pp. 18-19, 2013.

[13] Q. Luo, G. Cao, and J. Wang, "Sensorless permanent magnet synchronous motor vector control based on improved sliding mode observer," *Micro motor*, vol. 42, no. 3, pp. 55-63, 2014.

[14] R. Ren, L. Zhou, vic, "TMS320F28x source read," Beijing: electronic industry press, 2010:366-369.

BIOGRAPHIES

The Authors' photograph and biography not available at the time of publication.